The Standard Model of the Universe: The Effective Theory of Inflation. Warm Dark Matter from theory and galaxy observations.

H. J. de Vega

LPTHE, CNRS/Université P & M Curie (Paris VI).

15th Paris Cosmology Colloquium 2011

Observatoire de Paris, Paris campus

Wednesday 20, Thursday 21 and Friday 22 July 2011

- Begins by the inflationary era. Slow-Roll inflation explains horizon and flatness.

- Gravity is described by Einstein's General Relativity.

- Particle Physics described by the Standard Model of Particle Physics: $SU(3) \otimes SU(2) \otimes U(1) =$ qcd+electroweak model.

- Dark matter is non-relativistic during the matter dominated era where structure formation happens. DM is outside the SM of particle physics.

- Dark energy described by the cosmological constant Λ.

Standard Cosmological Model: ΛCDM $\Rightarrow$ ΛWDM

Dark Matter + Λ + Baryons + Radiation
begins by the Inflationary Era. Explains the Observations:

- Seven years WMAP data and further CMB data

- Light Elements Abundances

- Large Scale Structures (LSS) Observations. BAO.

- Acceleration of the Universe expansion:
  Supernova Luminosity/Distance and Radio Galaxies.

- Gravitational Lensing Observations

- Lyman α Forest Observations

- Hubble Constant and Age of the Universe
  Measurements

- Properties of Clusters of Galaxies

- Galaxy structure explained by WDM

The Theory of Inflation

Inflation can be formulated as an effective field theory in the Ginsburg-Landau sense. Main predictions:

- The inflation energy scale turns to be the grand unification energy scale: $= 0.70 \times 10^{16}$ GeV

- The MCMC analysis of the WMAP+LSS data combined with the effective theory of inflation yields: a) the inflaton potential is a double–well, b) the ratio r of tensor to scalar fluctuations. has the lower bound:
  $r > 0.023 \, (95\% \, \mathrm{CL}) \quad , \quad r > 0.046 \, (68\% \, \mathrm{CL})$ with
  $r \simeq 0.051$ as the most probable value.

This is borderline for the Planck satellite (early $2013?$) Burigana et. al. arXiv:1003.6108, ApJ 724, 588 (2010). D. Boyanovsky, C. Destri, H. J. de Vega, N. G. Sánchez, (review article), arXiv:0901.0549, Int.J.Mod.Phys.**A 24**, 3669-3864 (2009).

Dark Matter

DM particles can decouple being ultrarelativistic (UR) at $T_d \gg m$ or non-relativistic $T_d \ll m$.

We consider particles that decouple at or out of LTE (LTE = local thermal equilibrium).

Distribution function: $F_d[p_c]$ freezes out at decoupling.

p_c = comoving momentum.

$P_f(t) = p_c/a(t)$ = Physical momentum,

Velocity fluctuations: $\qquad Q = P_f(t)/T_d(t) = p_c/T_d$

$$\langle \vec{V}^2(t) \rangle = \langle \frac{\vec{P}_f^2(t)}{m^2} \rangle = \left[\frac{T_d}{m \, a(t)} \right]^2 \frac{\int_0^\infty Q^4 F_d(Q) dQ}{\int_0^\infty Q^2 F_d(Q) dQ} \; .$$

Energy Density: $\rho_{DM}(t) = \frac{m \, g}{2\pi^2} \frac{T_d^3}{a^3(t)} \int_0^\infty Q^2 \, F_d(Q) \, dQ$,

g : # of internal degrees of freedom of the DM particle, $1 \leq g \leq 4$. Formula valid at times when DM particles are non-relativistic.

Dark Matter density and DM velocity dispersion

Using entropy conservation: $T_d = \left(\frac{2}{g_d}\right)^{\frac{1}{3}} T_{cmb}$,

$g_d =$ effective $\#$ of UR degrees of freedom at decoupling,

$T_{cmb} = 0.2348 \; 10^{-3}$ eV, and

$$\frac{m \; g}{\pi^2 \; g_d} \; T_{cmb}^3 \int_0^\infty Q^2 \; F_d(Q) \; dQ = \rho_{DM}(\text{today}) = 1.107 \; \frac{\text{keV}}{\text{cm}^3} \; \text{(1)}$$

We obtain for the primordial velocity dispersion:

$$\sigma_{prim}(z) = \sqrt{\frac{1}{3} \; \langle \vec{V}^2 \rangle(z)} = 0.05124 \; \frac{1+z}{g_d^{\frac{1}{3}}} \left[\frac{\int_0^\infty Q^4 \; F_d(Q) \; dQ}{\int_0^\infty Q^2 \; F_d(Q) \; dQ}\right]^{\frac{1}{2}} \frac{\text{keV}}{m} \frac{\text{km}}{\text{s}}$$

Goal: determine m and g_d. We need TWO constraints.

Notice that $F_d(Q)$ and $I_{2n} = \int_0^\infty Q^{2n} \; F_d(Q) \; dQ$, $n = 1, 2$.

are quantities of order one.

The Phase-space density $Q = \rho/\sigma^3$ and its decrease factor Z

The phase-space density $Q \equiv \rho/\sigma^3$ is invariant under the cosmological expansion and can only decrease under self-gravity interactions (gravitational clustering).

The phase-space density today follows observing dwarf spheroidal satellite galaxies of the Milky Way (dSphs)

$$\frac{\rho_s}{\sigma_s^3} \sim 5 \times 10^3 \ \frac{\text{keV/cm}^3}{(\text{km/s})^3} = (0.18 \text{ keV})^4 \quad \text{Gilmore et al. 07 and 08.}$$

During structure formation $Q = \rho/\sigma^3$ decreases by a factor that we call $Z, \ (Z > 1)$:

$$Q_{today} = \frac{1}{Z} \ Q_{prim} \quad , \quad Q_{prim} = \frac{\rho_{prim}}{\sigma_{prim}^3} = \frac{3 \ \sqrt{3}}{2 \ \pi^2} \ g \ \frac{I_2^{\frac{5}{2}}}{I_4^{\frac{3}{2}}} \ m^4 \quad , \quad (2).$$

$$I_{2n} = \int_0^\infty Q^{2n} \ F_d(Q) \ dQ \quad , \quad n = 1, 2.$$

The spherical model gives $Z \simeq 41000$ and N-body simulations indicate: $10000 > Z > 1$. Z is galaxy dependent.

Mass Estimates for DM particles

Constraints: First $\rho_{DM}(\text{today})$, Second $Q_{today} = \rho_s/\sigma_s^3$

Combining the previous expressions lead to general formulas for m and g_d:

$$m = \frac{2^{\frac{1}{4}} \sqrt{\pi}}{3^{\frac{3}{8}} g^{\frac{1}{4}}} Z^{\frac{1}{4}} Q_{today}^{\frac{1}{4}} \frac{I_4^{\frac{3}{8}}}{I_2^{\frac{5}{8}}} , \; g_d = \frac{2^{\frac{1}{4}} g^{\frac{3}{4}}}{3^{\frac{3}{8}} \pi^{\frac{3}{2}} \Omega_{DM}} \frac{T_\gamma^3}{\rho_c} Q_{today}^{\frac{1}{4}} Z^{\frac{1}{4}} \left[I_2 \, I_4\right]^{\frac{3}{8}}$$

where: $Q_{today}^{\frac{1}{4}} = 0.18$ keV from the dSphs data,

$T_\gamma = 0.2348$ meV , $\Omega_{DM} = 0.228$, $\rho_c = (2.36 \text{ meV})^4$

These formulas yield for relics decoupling UR at LTE:

$$m = \left(\frac{Z}{g}\right)^{\frac{1}{4}} \text{keV} \begin{cases} 0.568 \\ 0.484 \end{cases} , \; g_d = g^{\frac{3}{4}} Z^{\frac{1}{4}} \begin{cases} 155 & \text{Fermions} \\ 180 & \text{Bosons} \end{cases} .$$

Since $g = 1 - 4$, we see that $g_d \gtrsim 100 \Rightarrow T_d \gtrsim 100$ GeV.

$1 < Z^{\frac{1}{4}} < 10$ for $1 < Z < 10000$. Example: for DM Majorana fermions $(g = 2)$ 0.5 keV $\lesssim m \lesssim 5$ keV.

Out of thermal equilibrium decoupling

Results for m and g_d on the same scales for DM particles decoupling UR out of thermal equilibrium.

For the χ model of sterile neutrinos where decoupling is out of thermal equilibrium:

$$0.56 \text{ keV} \lesssim m_\nu \, Z^{-\frac{1}{4}} \lesssim 1.0 \text{ keV} \quad , \quad 15 \lesssim g_d \, Z^{-\frac{1}{4}} \lesssim 84$$

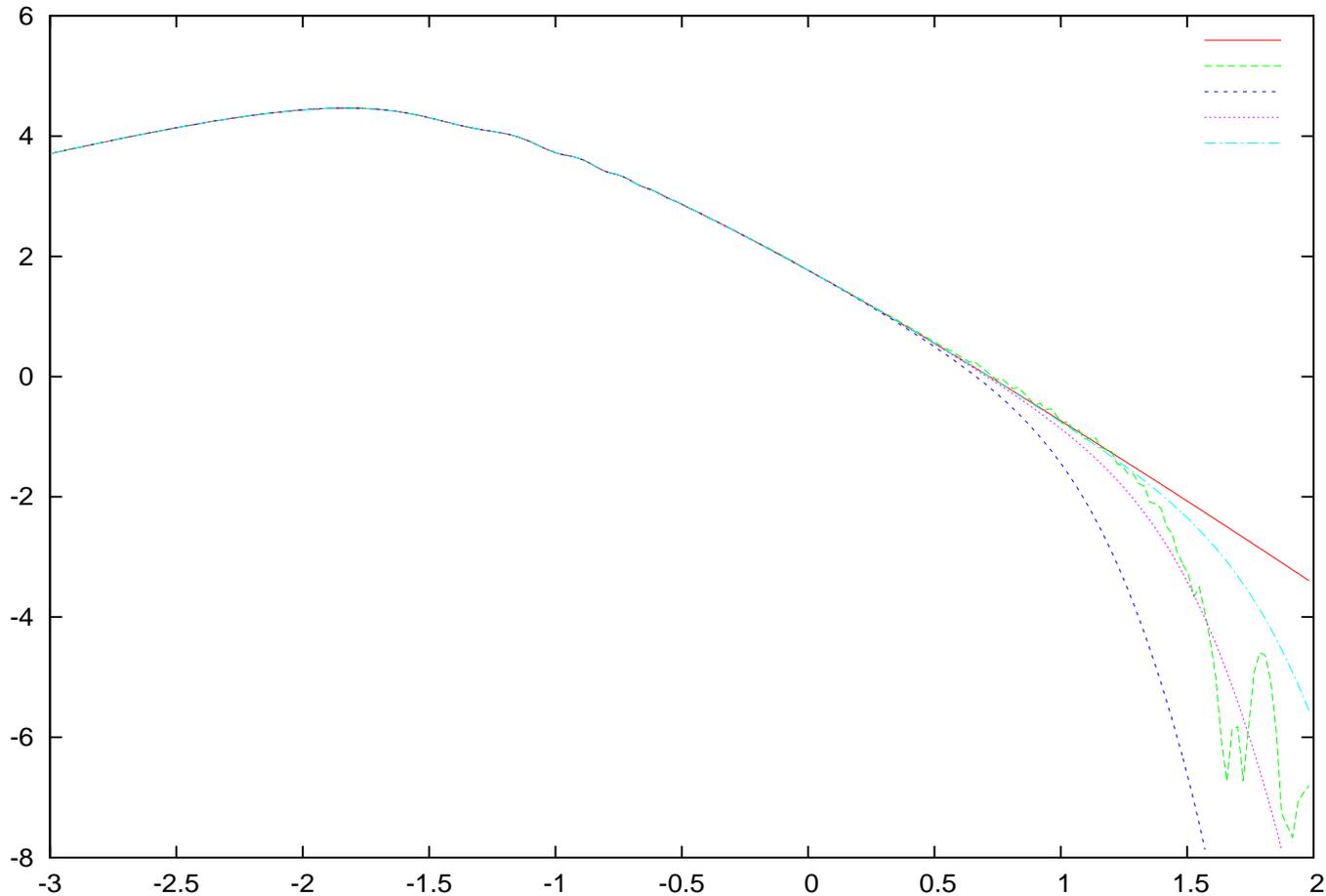Therefore, $0.6 \text{ keV} \lesssim m_\nu \lesssim 10 \text{ keV} \quad , \quad 20 \lesssim g_d \lesssim 850.$

Relics decoupling non-relativistic:
similar bounds: keV $\lesssim m \lesssim$ MeV

D. Boyanovsky, H. J. de Vega, N. Sanchez,
Phys. Rev. D 77, 043518 (2008), arXiv:0710.5180.

H. J. de Vega, N. G. Sanchez, MNRAS 404, 885 (2010),
arXiv:0901.0922.

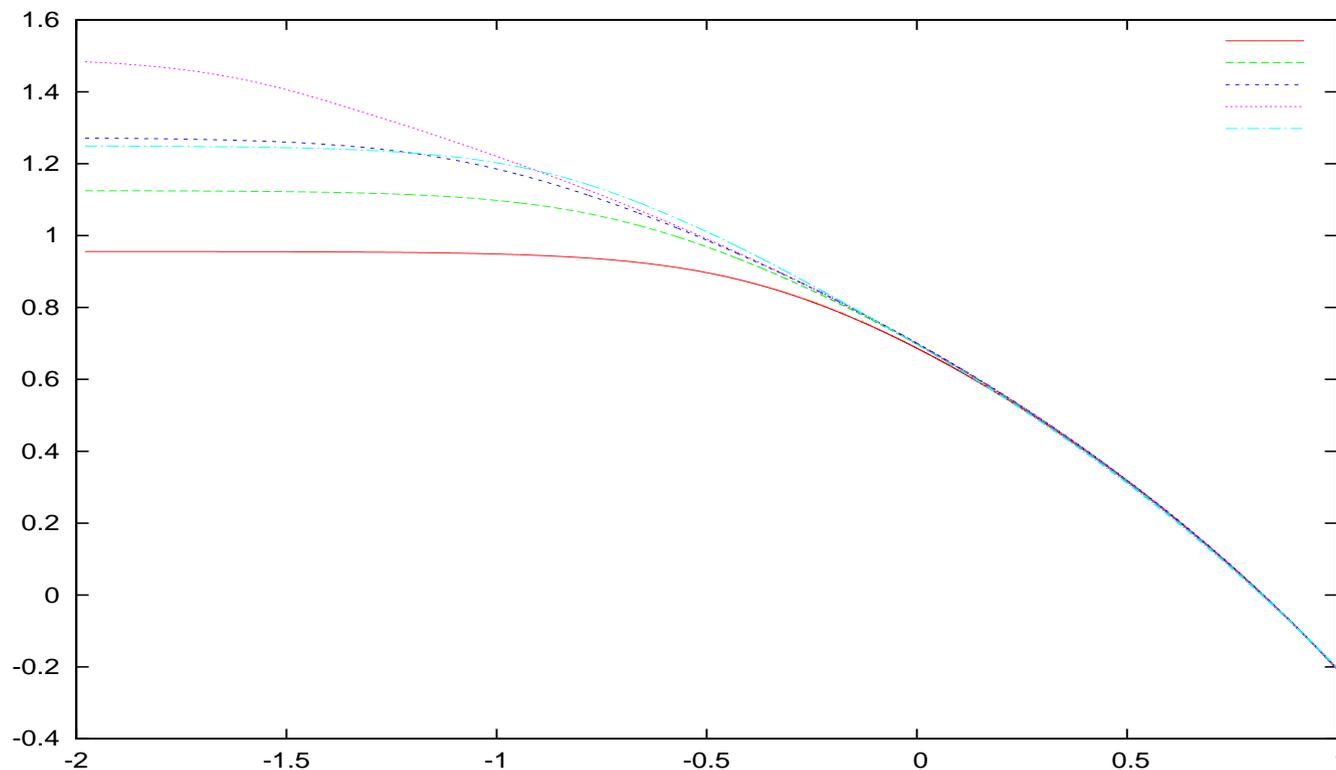# Linear primordial power today $P(k)$ vs. k Mpc h

$\log_{10} P(k)$ vs. $\log_{10}[k \text{ Mpc } h]$ for CDM, 1 keV, 2 keV, light-blue 4 keV DM particles decoupling in equil, and 1 keV sterile neutrinos. WDM cuts $P(k)$ on small scales

$$r \lesssim 100 \ (\text{keV}/m)^{4/3} \text{ kpc}$$

The expected overdensity

The expected overdensity within a radius R in the linear regime

$$\sigma^2(R) = \int_0^\infty \frac{dk}{k} \, \Delta^2(k) \, W^2(kR) \quad , \quad W(kR) : \text{window function.}$$
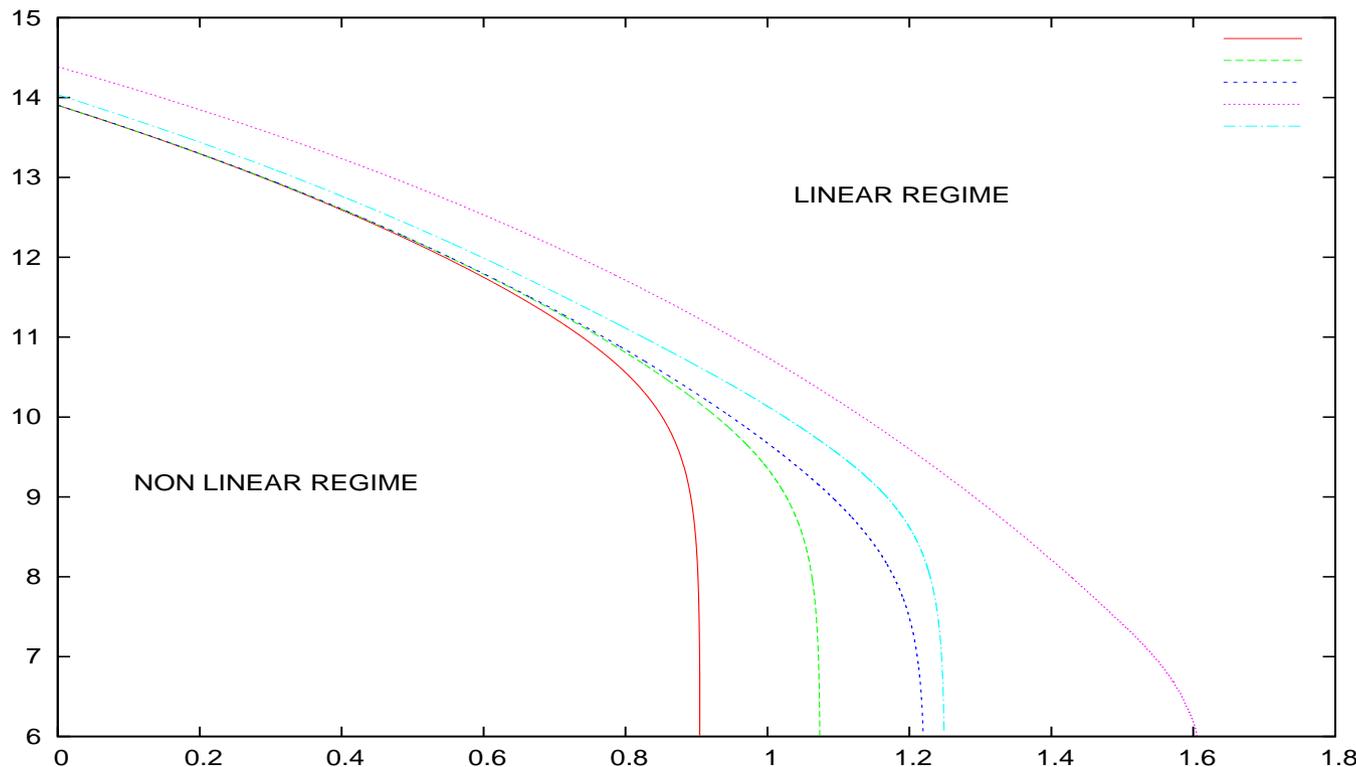

$\log \sigma(R)$ vs. $\log(R/h \, \mathrm{Mpc})$ for CDM, 1 keV, 2 keV, 4 keV DM particles decoupling in equil, and 1 keV (light-blue) sterile neutrinos.

WDM flattens and reduces $\sigma(R)$ for small scales.

Linear and non-linear regimes in z and R

$\sigma^2(R, z) \sim 1$: borderline between linear and non-linear regimes. Objects (galaxies) of scale R and mass $\sim R^3$ start to form when this scale becomes non-linear.
Smaller objects form earlier.

$\log M/M_\odot$ vs. $\log(z+1)$ for CDM, 1 keV, 2 keV, 4 keV DM particles decoupling in equil, and 1 keV (light-blue) sterile ν.

Galaxies

Physical variables in galaxies:

a) Nonuniversal quantities: mass, size, luminosity, fraction of DM, DM core radius r_0, central DM density ρ_0, ...

b) Universal quantities: surface density $\mu_0 \equiv r_0 \, \rho_0$ and DM density profiles. M_{BH}/M_{halo} (or the halo binding energy).

The galaxy variables are related by universal empirical relations. Only one variable remains free.

Universal quantities may be attractors in the dynamical evolution.

Universal DM density profile in Galaxies:

$$\rho(r) = \rho_0 \, F\left(\frac{r}{r_0}\right) \ , \ F(0) = 1 \ , \ x \equiv \frac{r}{r_0} \ , \ r_0 = \text{DM core radius.}$$

Empirical cored profiles: $F_{Burkert}(x) = \frac{1}{(1+x)(1+x^2)}$.

Cored profiles do reproduce the astronomical observations.

The constant surface density in DM and luminous galaxies

The Surface density for dark matter (DM) halos and for luminous matter galaxies defined as: $\mu_{0D} \equiv r_0 \, \rho_0$,

r_0 = halo core radius, ρ_0 = central density for DM galaxies

$$\mu_{0D} \simeq 120 \, \frac{M_\odot}{\text{pc}^2} = 5500 \, (\text{MeV})^3 = (17.6 \, \text{Mev})^3$$

5 kpc < r_0 < 100 kpc. For luminous galaxies $\rho_0 = \rho(r_0)$.
Donato et al. 09, Gentile et al. 09.[$\mu_{0D} = g$ in the surface].

Universal value for μ_{0D}: independent of galaxy luminosity for a large number of galactic systems (spirals, dwarf irregular and spheroidals, elliptics) spanning over 14 magnitudes in luminosity and of different Hubble types.

Similar values $\mu_{0D} \simeq 80 \, \frac{M_\odot}{\text{pc}^2}$ in interstellar molecular clouds of size r_0 of different type and composition over scales $0.001 \, \text{pc} < r_0 < 100$ pc (Larson laws, 1981).

Galaxy Surface Density

In the borderline $\sigma^2(R, z) = 1$ we can still use the linear theory. R is the scale of the region before it collapses.
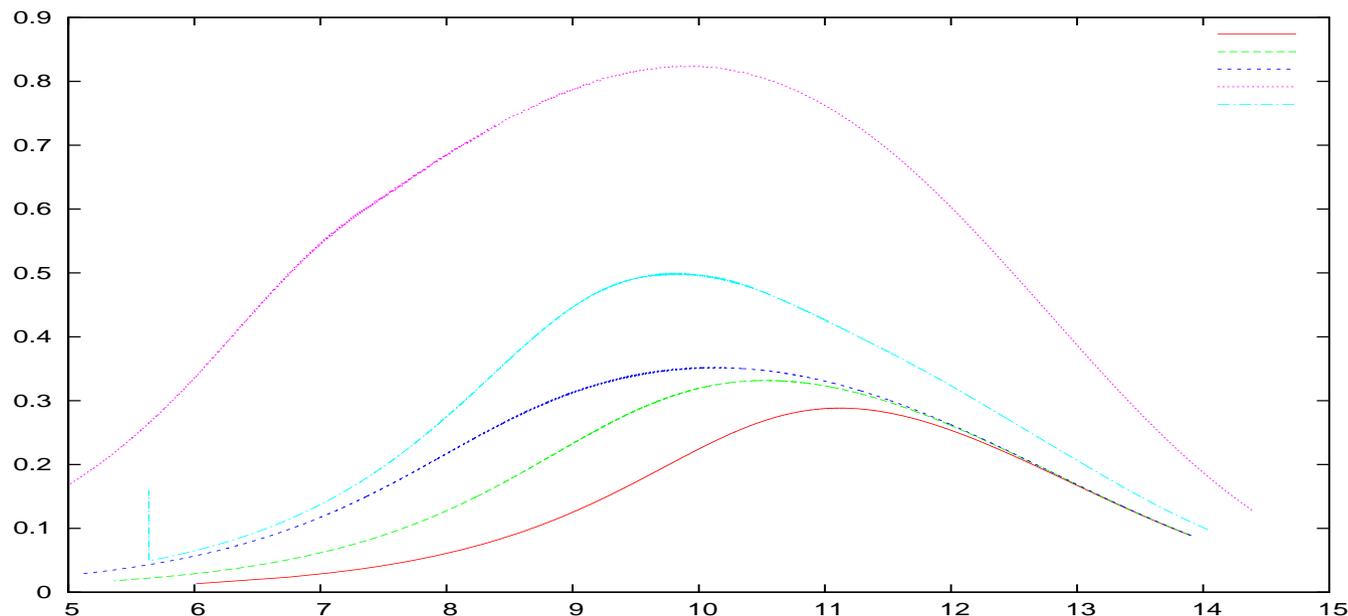
surface density μ in $M_\odot/\mathrm{pc}^2$ vs. $\log_{10} M/M_\odot$.

The surface density turns to vary less than one order of magnitude while the galaxy mass varies by 7-8 orders of magnitude.

CDM, 1 keV, 2 keV, 4 keV DM particles decoupling in equil, and 1 keV (light-blue) sterile neutrinos.

Scaling behind the approximately constant surface density

Mass $\sim \bar{\rho}_{DM} \, R^3 = 4 \times 10^{11} \, R^3 \, M_{\odot}$,

Surface density $\mu \sim \frac{M}{R_{phys}^2} = \frac{M}{R^2} \, (z+1)^2 \sim \bar{\rho}_{DM} \, R \, (z+1)^2$

$$\sigma^2(R, z) \simeq \sigma^2(R, 0)/(z+1)^2 \, , \; \sigma^2(R, z) = 1 \Rightarrow \sigma^2(R, 0) \simeq (z+1)^2$$

μ is approximately constant if $\sigma^2(R, 0) \sim 1/R$.

This scaling behaviour corresponds to spectral powers:
$$\Delta^2(k) \sim k \, , \; P(k) \sim 1/k^2 \, .$$

[This scaling is indeed valid in the relevant range
$.1 < k \, \mathrm{Mpc/h} < 3$ as shown by the plots.]

The spherical model gives in the non-linear regime

$\mu = \sqrt{\frac{8}{3\pi}} \, \mu_{lin} \, \left(\frac{\rho_0}{\bar{\rho}_{DM}} \right)^{\frac{5}{12}}$. Observations: $\rho_0/\bar{\rho}_{DM} \sim 3 \times 10^5$

$\mu \sim 200 \, \mu_{lin} \sim 50 - 90 \, M_{\odot}/\mathrm{pc}^2$ right order of magnitude !!

The Mass Function

The differential mass function gives the number of isolated bounded structures with mass between M and $M + dM$:
(Press-Schechter)

$$\frac{dN}{dM} = -\frac{2\,\delta_c}{\sqrt{2\,\pi}\,\sigma^2(M,z)}\,\frac{\rho_M(z)}{M^2}\,\frac{d\sigma(M,z)}{d\ln M}\,e^{-\delta_c^2/[2\,\sigma^2(M,z)]},$$
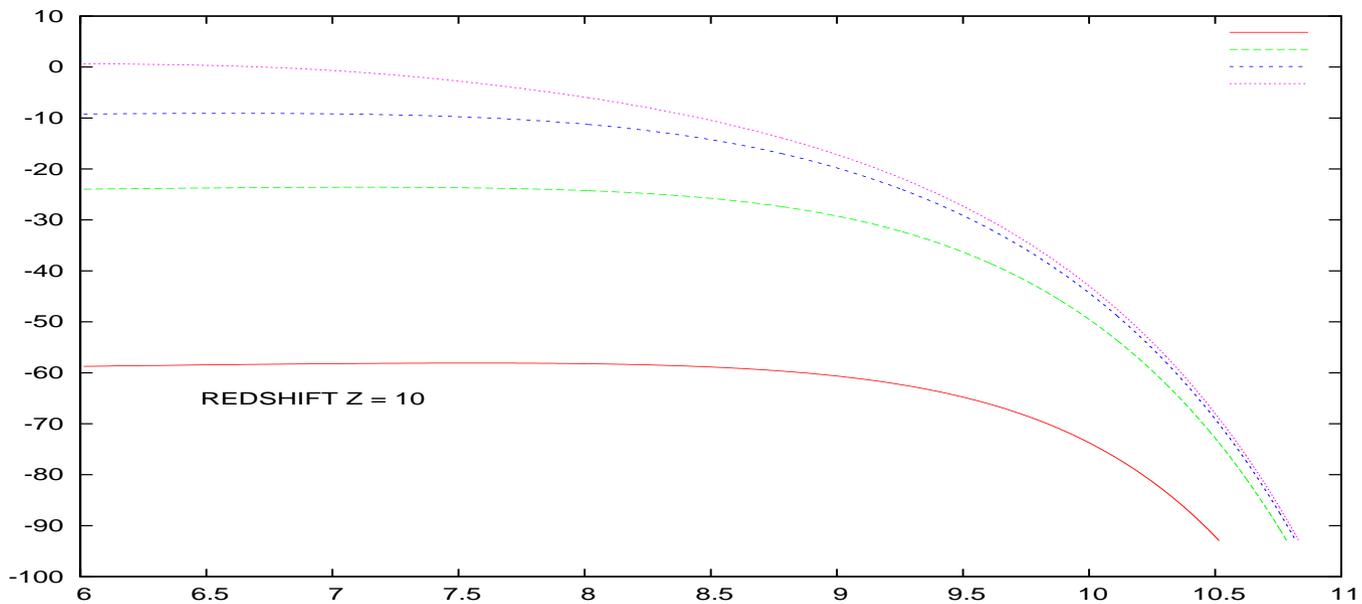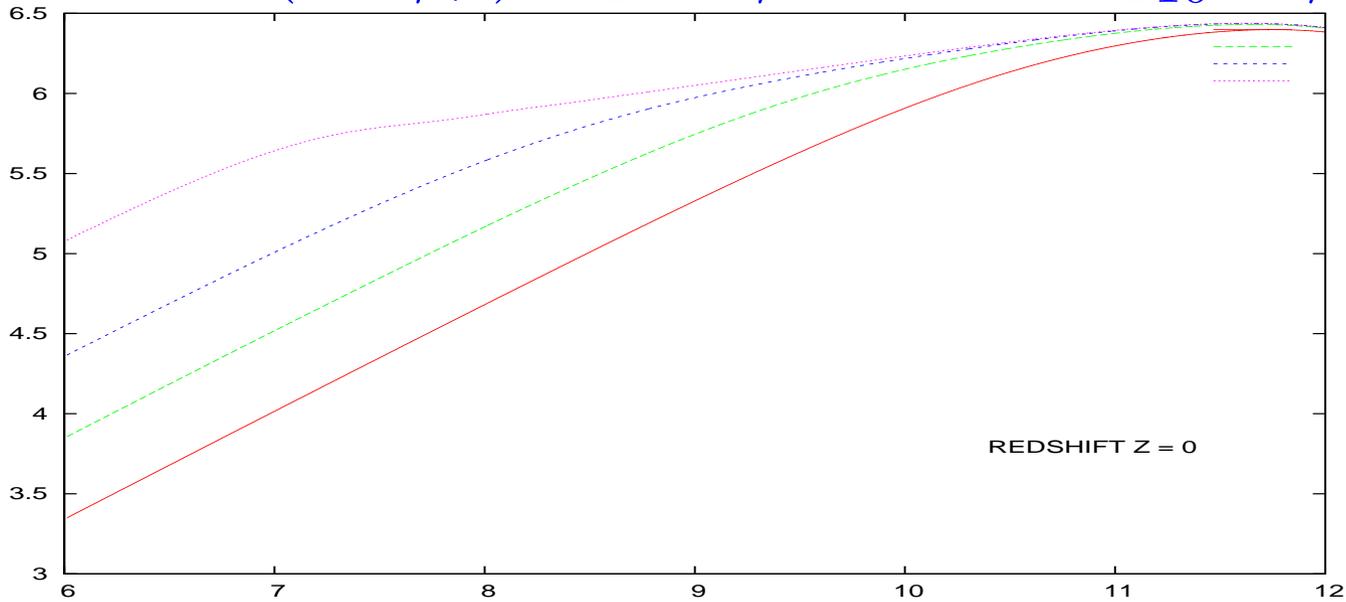
$\delta_c = 1.686\ldots$: linear estimate for collapse from the spherical model.

$\sigma(M,z)$ is constant for WDM for small scales: small objects (galaxies) formation is suppresed in WDM in comparison with CDM.

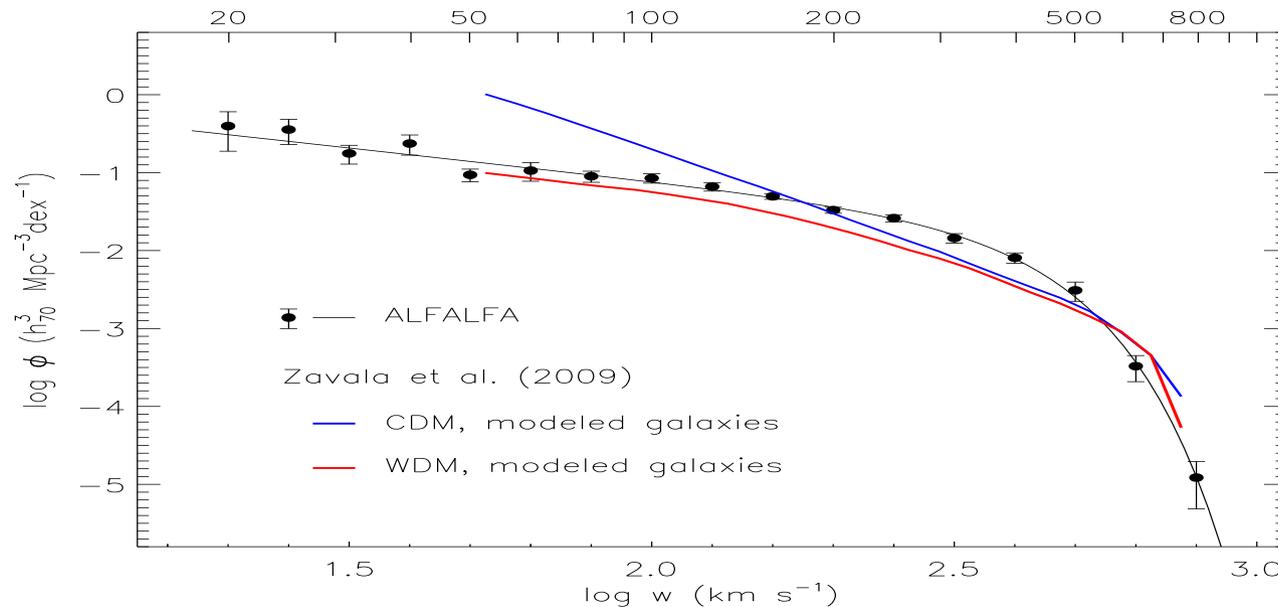$$\sigma(M,z) = \frac{g(z)}{z+1}\,\sigma(M,0) \quad \text{during the MD/}\Lambda \text{ dominated era.}$$

$g(z)$: takes into account the effect of the cosmological constant, $g(0) = 0.76$, $g(\infty) = 1$

$(M^2/\rho) \log dN/dM$ **vs.** $\log_{10} M/M_\odot$

REDSHIFT Z = 0

REDSHIFT Z = 10

CDM, 1 keV, 2 keV, 4 keV WDM decoupling in equilibrium.

Velocity widths in galaxies

Velocity widths in galaxies from 21cm HI surveys. ALFALFA survey clearly favours WDM over CDM. (Papastergis et al. 2011, Zavala et al. 2009).

Notice that the WDM red curve is for $m = 1$ keV WDM particle decoupling at thermal equilibrium.

The 1 keV WDM curve falls somehow below the data suggesting a slightly larger WDM particle mass.

WDM properties

WDM is characterized by

- its initial power spectrum cutted off for scales below ~ 50 kpc. Thus, structures are not formed in WDM for scales below ~ 50 kpc.

- its initial velocity dispersion. However, this is negligible for $z < 20$ where the non-linear regime starts.

N-body simulations show that structure formation happens later in WDM than in CDM since the non-linear regime starts later in WDM than in CDM (see previous viewgraph on that).

Structure formation is hierarchical in CDM.

WDM simulations show in addition top-hat structure formation at large scales and low densities but hierarchical structure formation remains dominant.
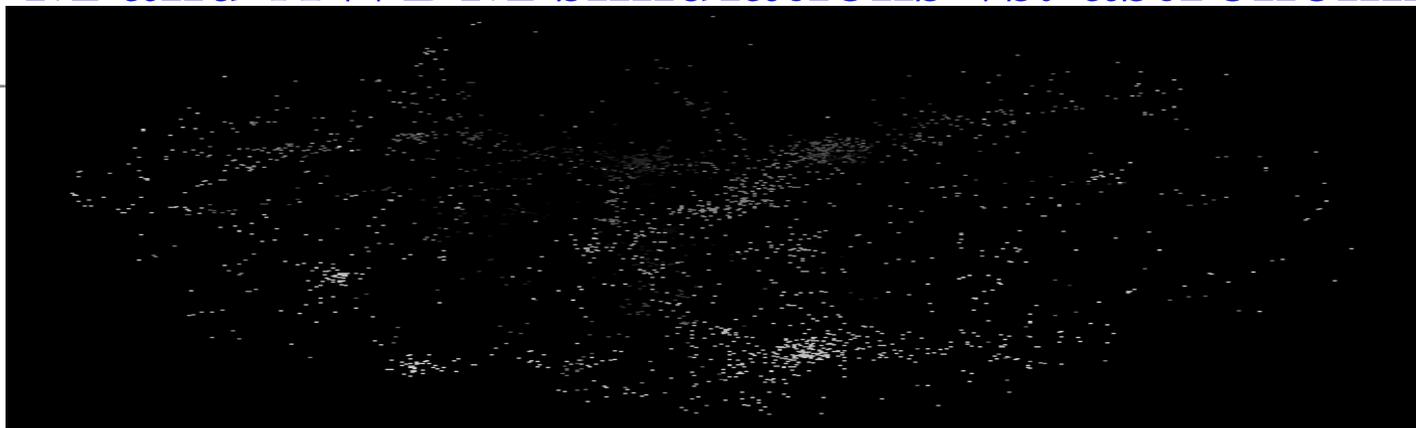
CDM

observations

1keV WDM

The distribution function of the decoupled DM particles:

$$f(\vec{x}, \vec{p}; t) = g\ f_0^{DM}(p) + F_1(\vec{x}, \vec{p}; t) \quad , \quad f_0^{DM}(p) = \text{zeroth order}$$

DM distribution function in or out of thermal equilibrium.

We evolve the distribution function $F_1(\vec{x}, \vec{p}; t)$ according to the linearized Boltzmann-Vlasov equation since the end of inflation. The DM density fluctuations are given by

$$\Delta(t, \vec{k}) \equiv m\ \int \frac{d^3 p}{(2\pi)^3}\ \int d^3 x\ e^{-i\,\vec{x}\cdot\vec{k}}\ F_1(\vec{x}, \vec{p}; t)$$

$$\Delta(z, \vec{k}) = \rho_{DM}\ \bar{\Delta}(z, k)\ \sqrt{V}\ |\phi_k|\ g(\vec{k})\ ,$$

where $\bar{\Delta}(z, k)$ obeys a Volterra integral equation,
the primordial inflationary fluctuations are:

$$|\phi_k| = \sqrt{2}\ \pi\ \frac{|\Delta_0|}{k^{\frac{3}{2}}}\ \left(\frac{k}{k_0}\right)^{\frac{n_s-1}{2}} \ ,\ g(\vec{k}) \text{ is a random gaussian field,}$$

$V = $ normalization phase-space volume.

$$|\Delta_0| \simeq 4.94\ 10^{-5},\ n_s \simeq 0.964,\ k_0 = 2\ \mathrm{Gpc}^{-1}\ ,\quad \text{WMAP7 .}$$

Linear density fluctuations today

The linearized Boltzmann-Vlasov equation can be recasted as a Volterra integral equation for the DM density fluctuations (de Vega, Sanchez, in preparation):

$\bar{\Delta}(z, k) =$

$h(z, k) + \frac{6}{(z+1) \, k \, r_{lin}} \, \int_{s_0}^{s} ds' \, \Pi\{k \, r_{lin}[s(z) - s']\} \, \bar{\Delta}(z(s'), k)$

$z(s) + 1 = (z_{eq} + 1) \, \sinh^2 s, \; z_{eq} + 1 \simeq 3200, \; \bar{\Delta}(\text{initial}, k) = 1$

$h(z, k) =$ known function: contains the memory from previous UR evolution and the photons gravitational potential.

$\Pi(x) \equiv \int_0^{\infty} Q \, dQ \, f_0^{DM}(Q) \, \sin(Q \, x) \, ,$

$f_0^{DM}(Q) =$ zeroth order freezed-out DM distribution.

This integral equation is valid both in the RD and MD eras as long as the DM particles are non relativistic. It becomes the Gilbert equation in the MD era (plus memory terms).

The Free Streaming Scale

The characteristic length scale is the free streaming scale (or Jeans' scale)

$$r_{lin} = 2\,\sqrt{1+z_{eq}}\,\left(\frac{3\,M_{Pl}^2}{H_0\,\sqrt{\Omega_{DM}}\,Q_{prim}}\right)^{\frac{1}{3}} = 21.1\,q_p^{-\frac{1}{3}}\ \text{kpc}$$

$q_p \equiv Q_{prim}/(\text{keV})^4$. DM particles can freely propagate over distances of the order of the free streaming scale.
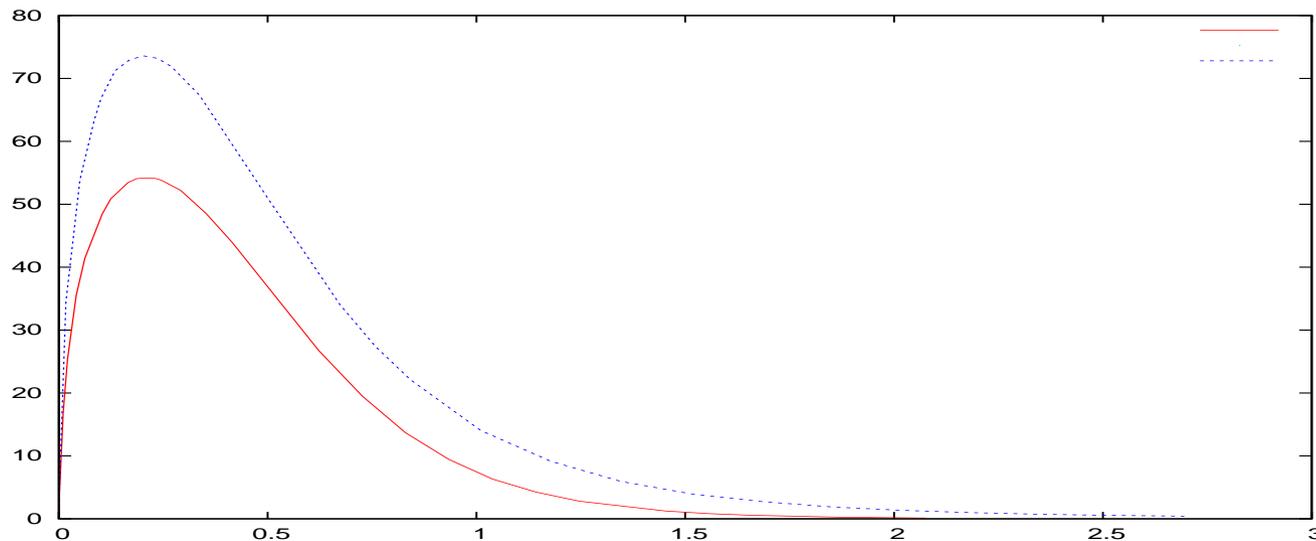
Transfer function $\bar{\Delta}(z=0,k)/\bar{\Delta}(\text{initial},k)$ vs. $k\,r_{lin}$. m = 1 keV. Red= thermal Fermi-Dirac. Blue = χ-sterile neutrinos.

Linear density profile

The matter density fluctuations $\rho_{lin}(r, z)$ are given at redshift z by

$$\rho_{lin}(r, z) = \frac{1}{2\pi^2 r} \int_0^\infty k \, dk \, \sin(k\,r) \, \Delta(k, z) \quad \text{for} \quad g(\vec{k}) = 1$$

The linear profile today results:

$$\rho_{lin}(x) = 0.034 \, \rho_{DM} \, \frac{q_p^{\frac{n_s+2}{3}}}{x} \, I_3 \int_0^\infty \gamma^{n_s/2-1} \, d\gamma \, \sin(\gamma\,x) \, \bar{\Delta}(z, \gamma)$$
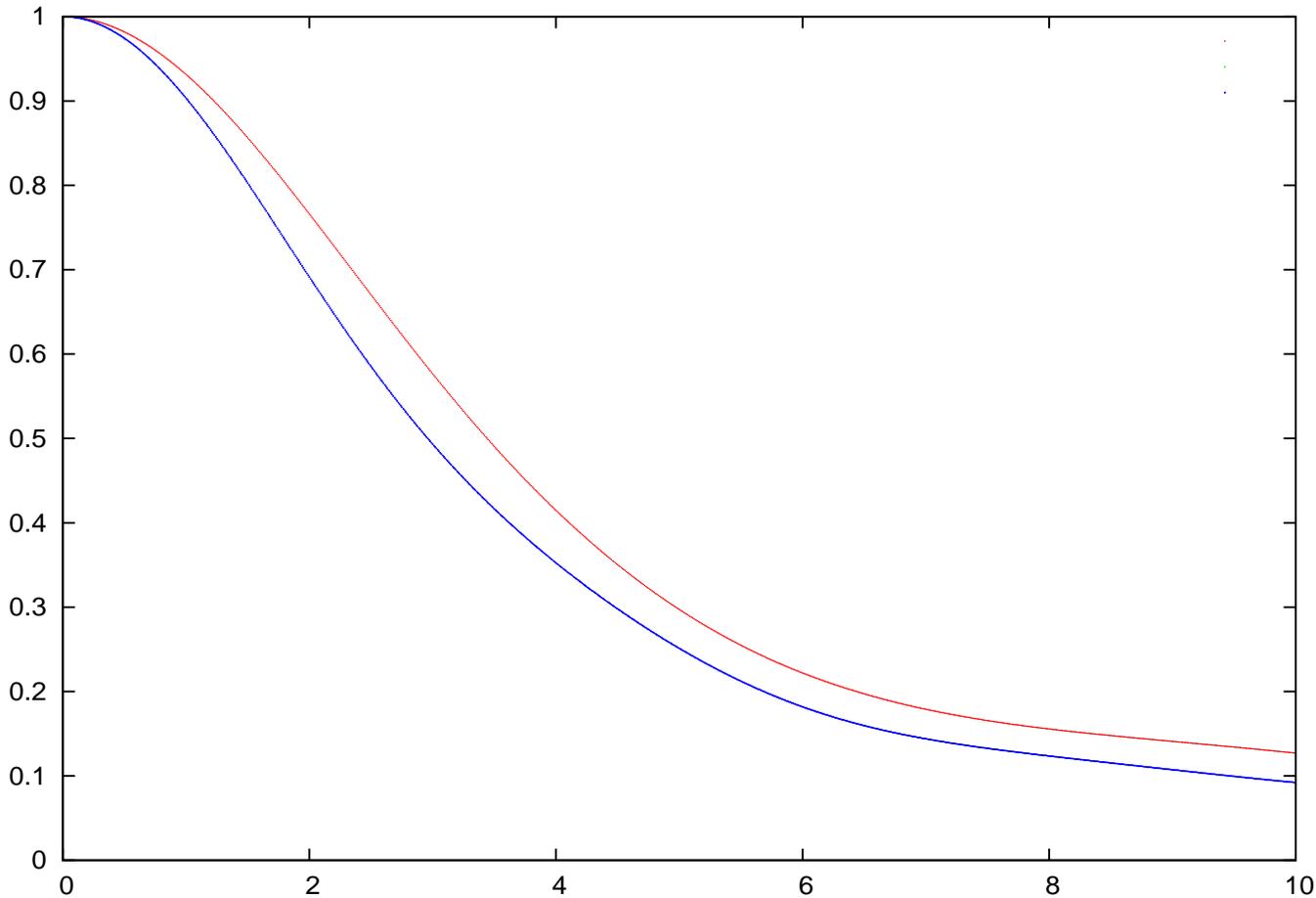
where $\gamma \equiv k \, r_{lin}$ and $x \equiv r/r_{lin}$.

I_n and $\bar{\Delta}(z, \gamma)$ depend on the freezed-out DM distribution $f_0^{DM}(Q)$.

Notice that $\quad \bar{\Delta}(z, \gamma) \simeq \frac{1}{z+1} \, \bar{\Delta}(0, \gamma)$

Therefore, the profile shape turns to be redshift independent in the MD/Λ era.

Density profiles in the linear approximation

Profiles $\rho_{lin}(r)/\rho_{lin}(0)$ vs. $x \equiv r/r_{lin}$.

Fermions decoupling ultrarelativistically in and out of thermal equilibrium. The halo radius r_0 is proportional to r_{lin}: $r_0 = \beta\, r_{lin}$. $\quad \beta_{in\,equil} = 5.565$, $\beta_{out\,equil} = 5.013$.

Density profiles in the linear approximation

Density profiles turn to be cored at scales $r \ll r_{lin}$.

Intermediate regime $r \gtrsim r_{lin}$:

$$\rho_{lin}(r) \overset{r \gtrsim r_{lin}}{=} c_0 \left(\frac{r_{lin}}{r}\right)^{1+n_s/2} \rho_{lin}(0) \quad , \quad 1 + n_s/2 = 1.482.$$

$\rho_{lin}(r)$ scales with the primordial spectral index n_s.

The theoretical linear results agree with the universal empirical behaviour $r^{-1.6 \pm 0.4}$: M. G. Walker et al. (2009) (observations), I. M. Vass et al. (2009) (simulations).

The agreement between the linear theory and the observations is remarkable.

In the asymptotic regime $r \gg r_{lin}$ the small k behaviour of

$$\Delta(k, t_{\text{today}}) \overset{k \to 0}{=} c_1 (k \, r_{lin})^s$$ with $s \simeq 0.5$ implies the presence

of a tail: $\quad \rho_{lin}(r) \overset{r \gg r_{lin}}{\simeq} c \left(\frac{r_{lin}}{r}\right)^2.$

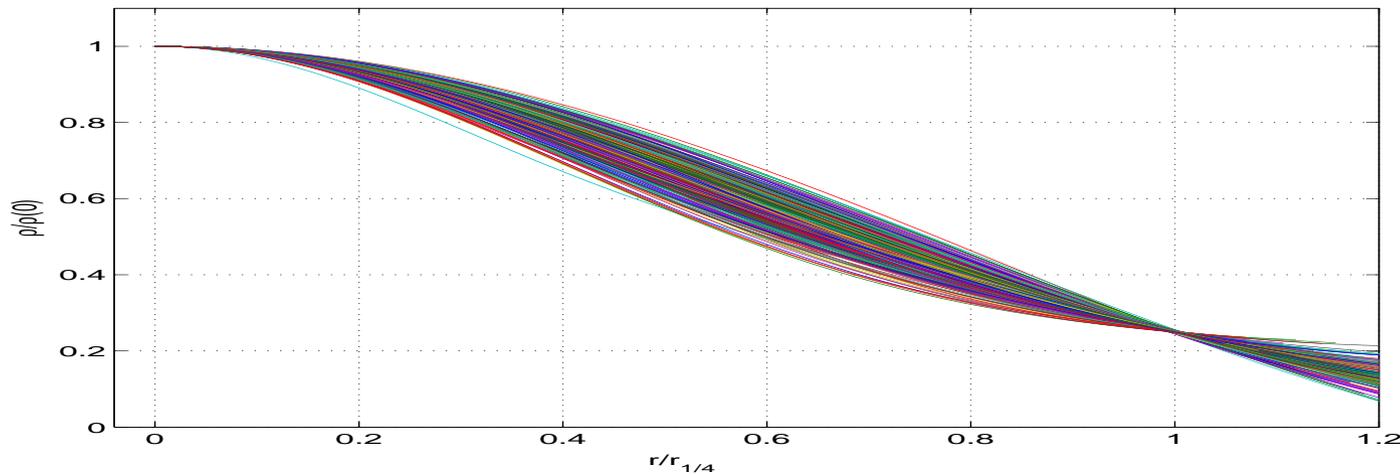# Linear CDM profiles are cusped
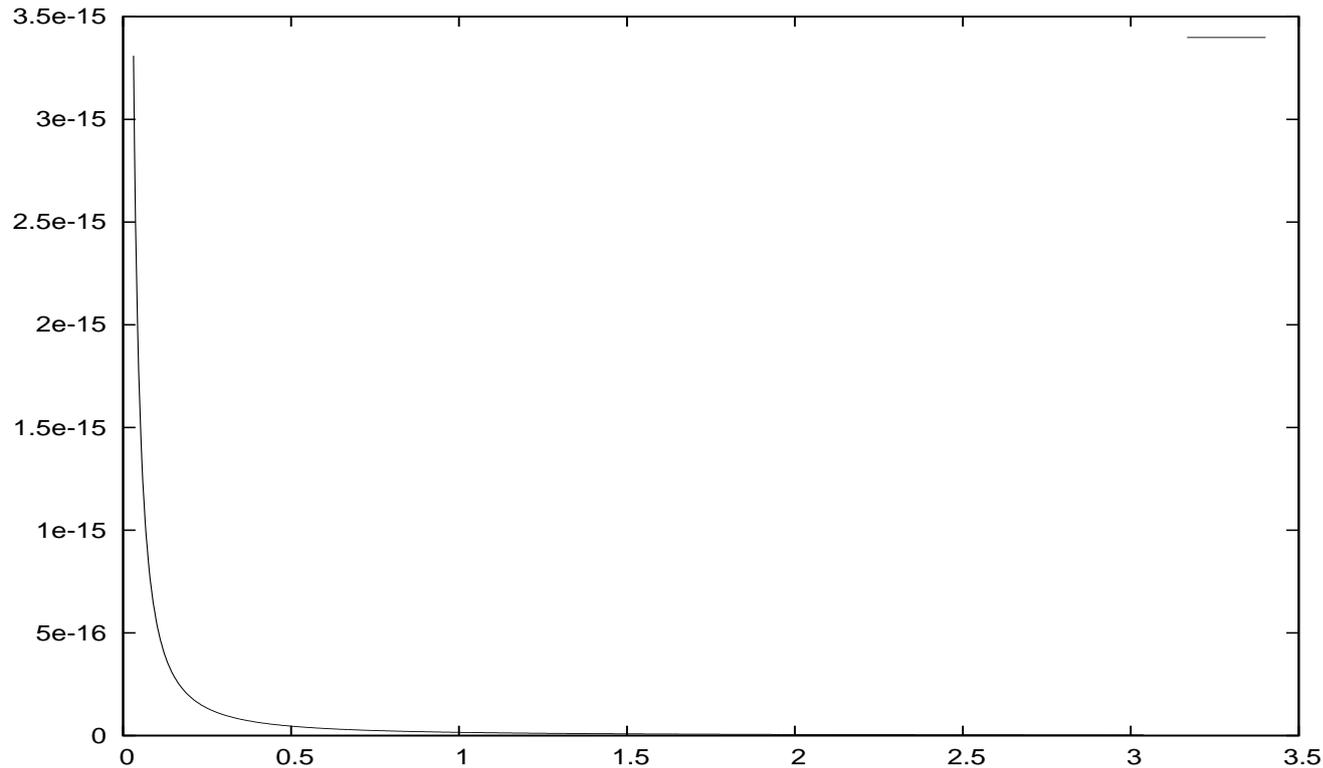
$\rho_{lin}(r)_{CDM}$ in g/cm^3 vs. r in pc.

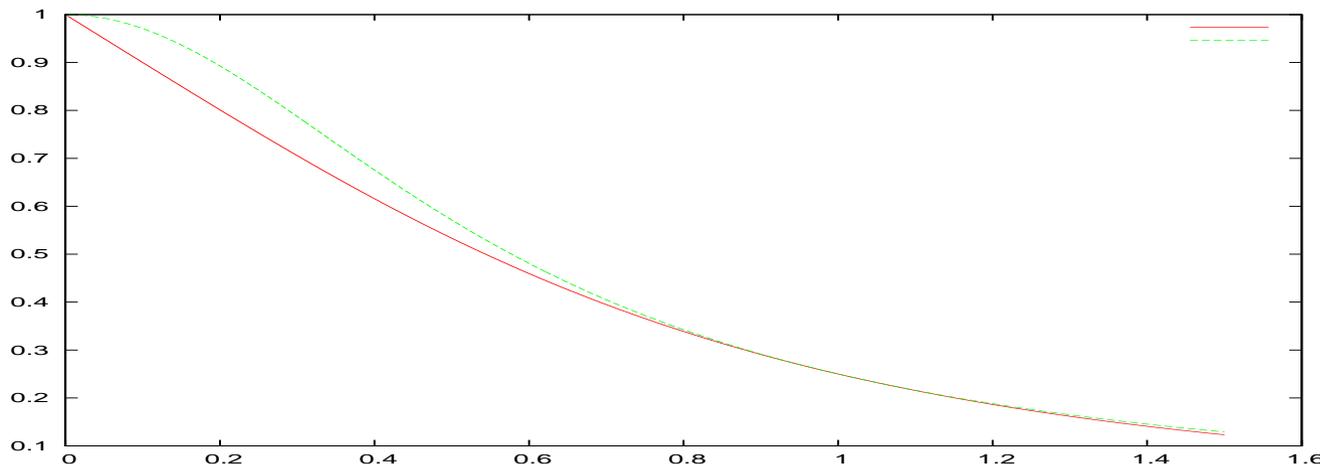Exhibits a cusp behaviour for $r \gtrsim 0.03$ pc.

(Here $m_{CDM} = 100$ GeV).

Observations in DM dominated galaxies always find cores.

Linear evolution from random initial conditions
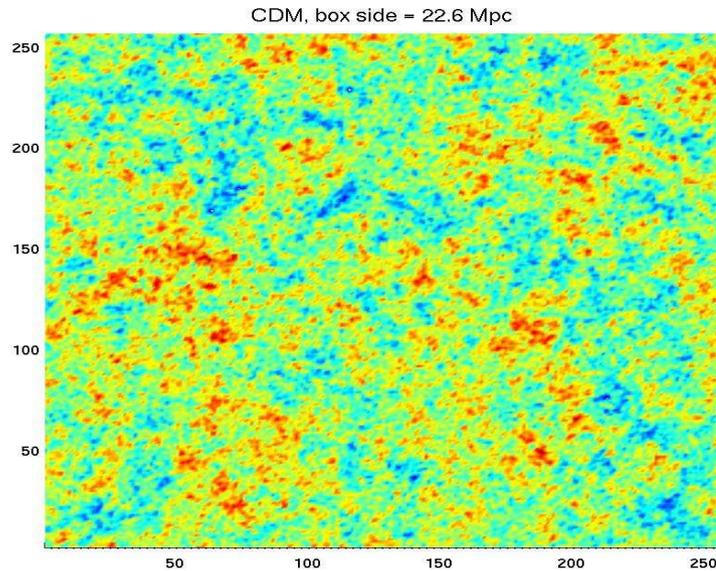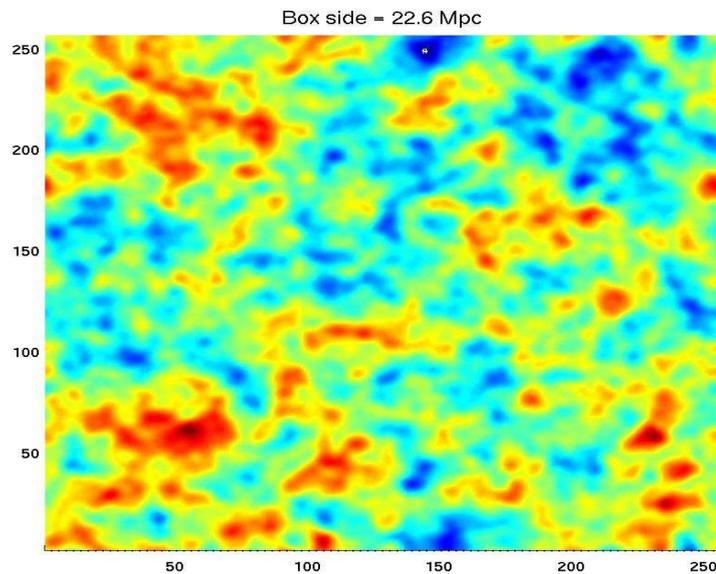

Profiles averaged in the angles for 500 random initial conditions. $\rho(r)/\rho(0)$ vs. $r/r_{1/4}$ [Destri, de Vega, Sanchez, in preparation]. Burkert and Pseudothermal profiles $\rho(r)/\rho(0)$ vs. $r/r_{1/4}$.

WDM vs. CDM linear fluctuations today

CDM, box side = 22.6 Mpc

Box side = 22.6 Mpc. [Destri, de Vega, Sanchez, in preparation]

Box side = 22.6 Mpc

Particle physics candidates for DM

No particle in the Standard Model of particle physics (SM) can play the role of DM.

Many extensions of the SM can be envisaged to include a DM particle with mass in the keV scale and weakly enough coupled to the Standard Model particles to fulfill all particle physics experimental constraints.

Main candidates in the keV mass scale: sterile neutrinos, gravitinos, light neutralino, majoron ...

Particle physics motivations for sterile neutrinos:

There are both left and right handed quarks (with respect to the chirality).

It is natural to have right handed neutrinos ν_R besides the known left-handed neutrino. Quark-lepton similarity.

Sterile Neutrinos in the SM of particle physics

SM symmetry group: $SU(3)_{color} \otimes SU(2)_{weak} \otimes U(1)^{weak}_{hypercharge}$

Leptons are color singlets and doublets under weak SU(2).

Sterile neutrinos ν_R do not participate to weak interactions. Hence, they must be singlets of color, weak SU(2) and weak hypercharge.

The SM Higgs Φ is a SU(2) doublet with a nonzero vacuum expectation value Φ_0. It can couple Yukawa-type with the left and right handed leptons:

$$L_{Yuk} = y\, \bar{\nu}_L\, \nu_R\, \Phi_0 + h.c. \quad ,$$

$y =$ Yukawa coupling, $\quad \Phi_0 = \begin{pmatrix} 0 \\ v \end{pmatrix} \quad , \quad v = 174$ GeV.

This induces a mixing (bilinear) term between ν_L and ν_R which produces transmutations of $\nu_L \Leftrightarrow \nu_R$.

Sterile Neutrinos Mixing

Mixing and oscillations of particle states are typical of low energy particle physics !

- Flavor mixing: e-μ neutrino oscillations (explain solar neutrinos).

- $K^0 - \overline{K}^0$, $B^0 - \overline{B}^0$ and $D^0 - \overline{D}^0$ meson oscillations in connection with CP-violation.

Neutrino mass matrix: $(\bar{\nu}_L \ \bar{\nu}_R) \begin{pmatrix} 0 & m_D \\ m_D & M \end{pmatrix} \begin{pmatrix} \nu_L \\ \nu_R \end{pmatrix}$

$M =$ right-neutrino mass, $m_D = y \, v$, $M \gg m_D$. Seesaw.

Mass eigenvalues: $\frac{m_D^2}{M}$ and M, with eigenvectors:

- active neutrino: $\nu_{active} \simeq \nu_L - \frac{m_D}{M} \, \nu_R$.

- sterile neutrino: $\nu_{sterile} \simeq \nu_R + \frac{m_D}{M} \, \nu_L, \quad M \gg m_D^2/M$.

Sterile Neutrinos

Choosing $M \sim 1$ keV and $m_D \sim 0.1$ eV is consistent with observations.

Mixing angle: $\theta \sim \frac{m_D}{M} \sim 10^{-4}$ is appropriate to produce enough sterile neutrinos accounting for the observed DM.

Smallness of θ makes sterile neutrinos difficult to detect.

Precise measure of nucleus recoil in tritium beta decay: $^3H_1 \Longrightarrow {}^3He_2 + e^- + \bar{\nu}$ can show the presence of a sterile instead of the active $\bar{\nu}$ in the decay products.

Rhenium 187 beta decay gives $\theta < 0.095$ for 1 keV steriles [Galeazzi et al. PRL, 86, 1978 (2001)].
Available energy: $Q(^{187}Re) = 2.47$ keV, $Q(^3H_1) = 18.6$ keV.

Conclusion: the empty slot of right-handed neutrinos in the Standard Model of particle physics can be filled by keV-scale sterile neutrinos describing the DM.

MARE searchs sterile neutrinos in beta decay

Heavy neutrinos limits from past ^{187}Re experiments / 2

MANU (M. Galeazzi et al., Phys. Rev. Lett. 86, 1978 (2001))
MIBETA (preliminary, unpublished)
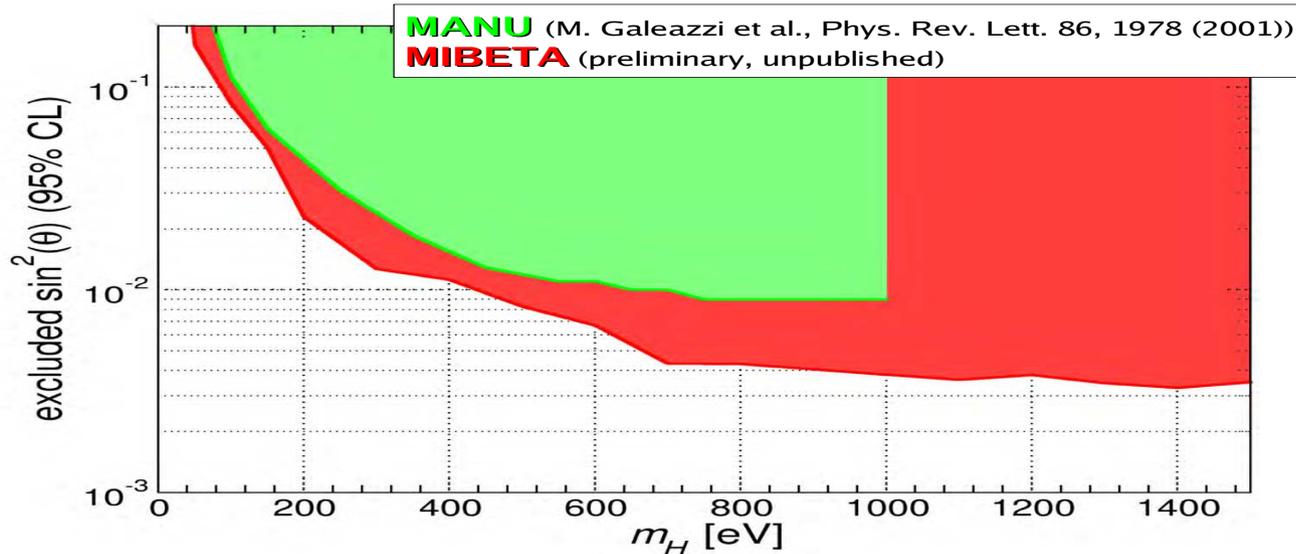
A. Nucciotti, Meudon Workshop 2011, 8-10 JUNE 2011   35

MARE sensitivity to heavy neutrinos: ^{187}Re option

Legend:
- $N_{ev} = 10^{14}$, $\Delta E = 1.5$ eV, $f_{pp} = 10^{-6}$
- $N_{ev} = 10^{13}$, $\Delta E = 5$ eV, $f_{pp} = 10^{-5}$
- $N_{ev} = 10^{12}$, $\Delta E = 30$ eV, $f_{pp} = 10^{-4}$

light ν sensitivities:
$m_\nu < 1$ eV
$m_\nu < 0.35$ eV
$m_\nu < 0.1$ eV
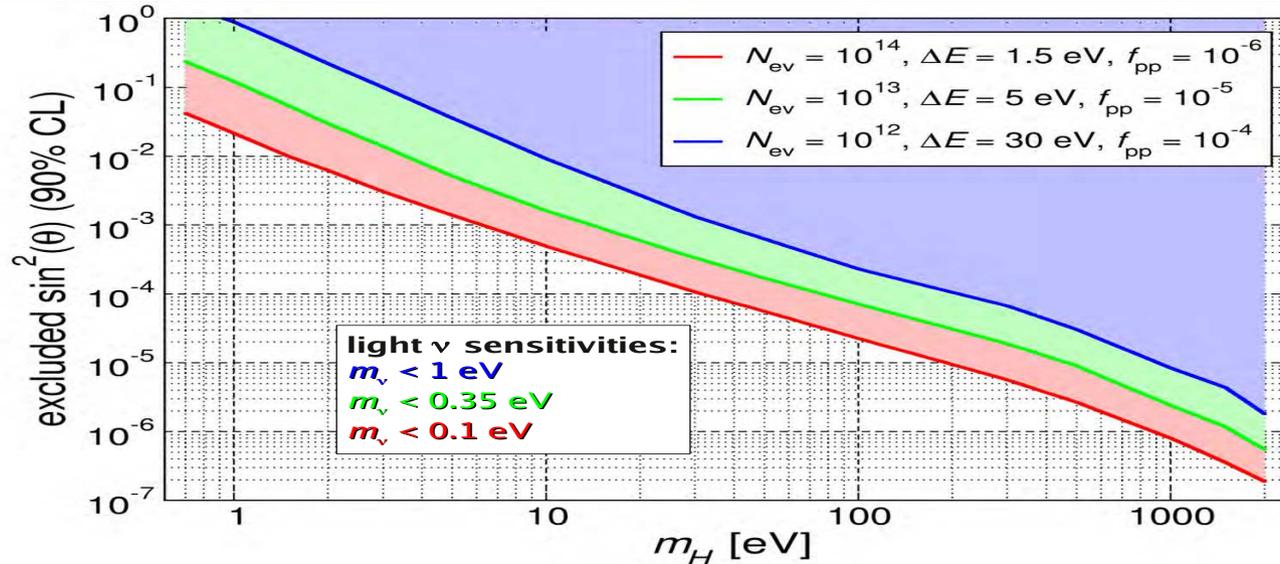
A. Nucciotti, Meudon Workshop 2011, 8-10 JUNE 2011   36

Sterile neutrino models

Sterile neutrinos: named by Bruno Pontecorvo (1968).

- DW: Dodelson-Widrow model (1994) sterile neutrinos produced by non-resonant mixing from active neutrinos.

- Shi-Fuller model (1998) sterile neutrinos produced by resonant mixing from active neutrinos.

- χ-model (1981)-(2006) sterile neutrinos produced by a Yukawa coupling from a real scalar χ.

- Further models must reproduce $\bar{\rho}_{DM}$, galaxy and structure formation and be consistent with particle physics experiments.

WDM decoupling out of equilibrium behave approximately as particles decoupling at equilibrium but with a larger mass: $m_{DW} \simeq 4.4 \, (m_{Thermal})^{4/3}$, $m_{SF} \simeq 3 \, m_{\chi}$, $m_{DW} \simeq 1.5 \, m_{SF}$. Linear information: $\bar{\rho}_{DM}$ and free-streaming length.

Summary: keV scale DM particles

- Reproduce the phase-space density observed in dwarf satellite galaxies and spiral galaxies (dV S 2009).

- Provide cored universal galaxy profiles in agreement with observations (dV S 2009,dV S S 2010). (Review on cores vs. cusps by de Blok 2010, Salucci & Frigerio Martins 2009)

- Reproduce the universal surface density μ_0 of DM dominated galaxies (dV S S 2010). WIMPS simulations give 1000 times the observed value of μ_0 (Hoffman et al. 2007).

- Alleviate the satellite problem which appears when wimps are used (Avila-Reese et al. 2000, Götz & Sommer-Larsen 2002, Markovic et al. 2011)

- Alleviate the voids problem which appears when wimps are used (Tikhonov et al. 2009).

Summary: keV scale DM particles

- All direct searches of DM particles look for $m \gtrsim 1$ GeV. DM mass in the keV scale explains why nothing has been found ... e^+ and $\bar{p}$ excess in cosmic rays may be explained by astrophysics: P. L. Biermann et al. (2009), P. Blasi, P. D. Serpico (2009).

- Galaxies from Wimps simulations are too small (Ryan Joung et al. 2009, Holz & Perlmutter 2010). keV scale DM may alleviate this problem.

- Velocity widths in galaxies from 21cm HI surveys. ALFALFA survey clearly favours WDM over CDM. Papastergis et al. 2011, Zavala et al. 2009

Extensive and reliable simulations with keV mass DM are needed to clarify all these issues.

Summary and Conclusions

● Combining theoretical evolution of fluctuations through the Boltzmann-Vlasov equation with galaxy data points to a DM particle mass 3 - 10 keV. T_d turns to be model dependent. The keV mass scale holds independently of the DM particle physics model.

● Universal Surface density in DM galaxies $[\mu_{0D} \simeq (18 \ \mathrm{MeV})^3]$ explained by keV mass scale DM. Density profile scales and decreases for intermediate scales with the spectral index $n_s : \ \rho(r) \sim r^{-1-n_s/2}$ and $\rho(r) \sim r^{-2}$ for $r \gg r_0$.

H. J. de Vega, P. Salucci, N. G. Sanchez, 'The mass of the dark matter particle from theory and observations', arXiv:1004.1908.

H. J. de Vega, N. Sanchez, 'Model independent analysis of dark matter points to a particle mass at the keV scale', arXiv:0901.0922, MNRAS 404, 885 (2010).

Future Perspectives

The Golden Age of Cosmology and Astrophysics continues.

Galaxy and Star formation. DM properties from galaxy observations. Early star formation. Gigantic AGN black-holes and their correlation with galaxy evolution.

Chandra, Suzaku X-ray data: keV mass DM decay? The Dark Ages...Reionisation...the 21cm line...

Sun models well reproduce the sun's chemical composition but not the heliosismology (Asplund et al. 2009).
Can DM inside the Sun help to explain the discrepancy?
Nature of Dark Matter? 83% of the matter in the universe.
Light DM particles are strongly favoured $m_{DM} \sim$ keV.
Sterile neutrinos ? Other particle in the keV mass scale?
Precision determination of DM properties (mass, T_d, nature) from better galaxy data combined with theory (Boltzmann-Vlasov and simulations).

The Universe is our ultimate physics laboratory

THANK YOU VERY MUCH

FOR YOUR ATTENTION!!

Scaling of the energy and entropy from the surface density

Total energy using the virial and the profile $F(x)$:

$$E = \tfrac{1}{2} \langle U \rangle = -\tfrac{1}{4}\, G\, \int \frac{d^3r\; d^3r'}{|\boldsymbol{r}-\boldsymbol{r}'|}\, \langle \rho(r)\, \rho(r') \rangle =$$

$$= -\tfrac{1}{4}\, G\, \rho_0^2\, r_0^5 \int \frac{d^3x\; d^3x'}{|\boldsymbol{x}-\boldsymbol{x}'|}\, \langle F(x)\, F(x') \rangle \quad \Rightarrow \quad E \sim G\, \mu_{0D}^2\, r_0^3$$

The energy scales as the volume.

For consistency with the profile, the Boltzmann-Vlasov distribution function must scale as

$$f(\boldsymbol{p}, \boldsymbol{r}) = \frac{1}{m^4\; r_0^3\; G^{\frac{3}{2}}\; \sqrt{\rho_0}}\; \mathcal{F}\left(\frac{\boldsymbol{p}}{m\; r_0\; \sqrt{G\, \rho_0}}, \frac{\boldsymbol{r}}{r_0} \right)$$

Hence, the entropy scales as

$$S = \int f(\boldsymbol{p}, \boldsymbol{r})\; \log f(\boldsymbol{p}, \boldsymbol{r})\; d^3p\; d^3r \;\sim\; r_0^3\, \frac{\rho_0}{m} \;=\; r_0^2\, \frac{\mu_{0D}}{m}\;.$$

The entropy scales as the surface (as for black-holes). However, very different proportionality coefficients:

$\frac{S_{BH}/A}{S_{gal}/r_0^2} \sim \frac{m}{\text{keV}}\, 10^{36} \Rightarrow$ Much smaller coefficient for galaxies than for black-holes. Bekenstein bound satisfied.

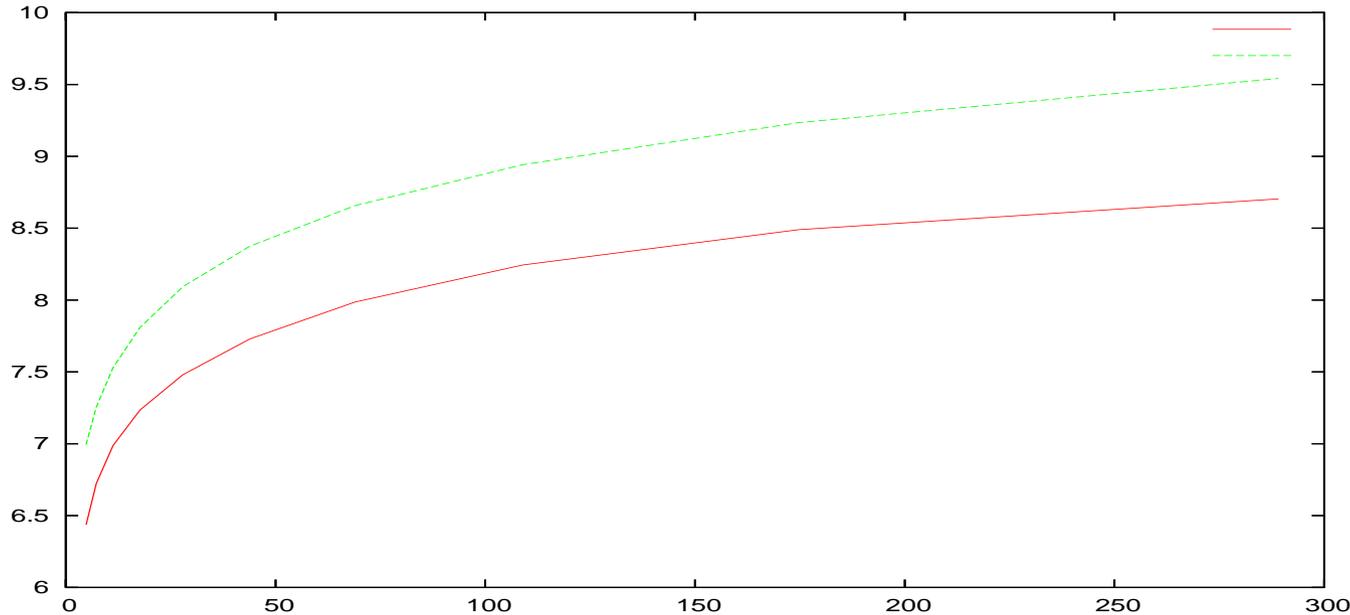# ρ/σ^3 vs. r for different z from ΛCDM simulations
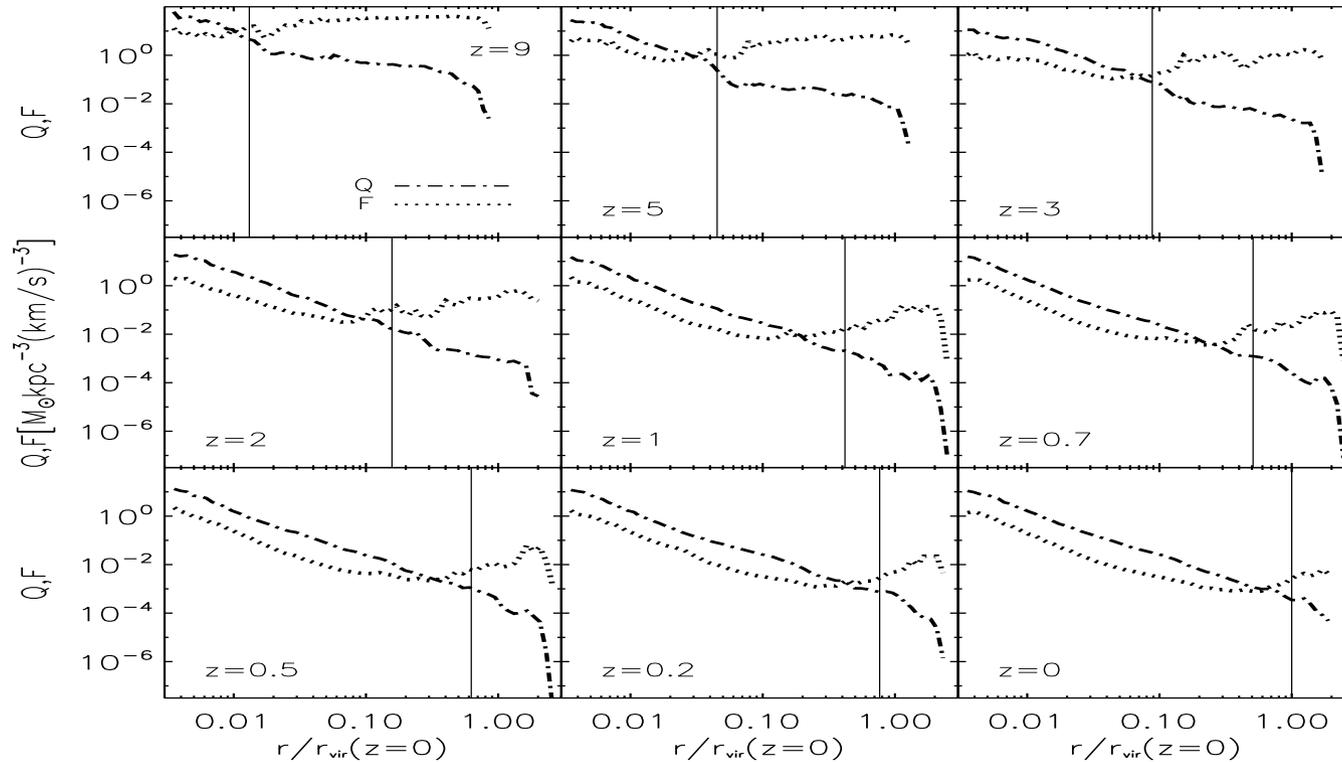
Phase-space density $Q \equiv \rho/\sigma^3$ vs. $r/r_{vir}(z=0)$ dot-dashed line for different redshifts: $0 \le z \le 9$.

We see that from $z=9$ to $z=0$ the r-average of ρ/σ^3 decreases by a factor $Z \sim 10$.

I. M. Vass et al. MNRAS, 395, 1225 (2009).

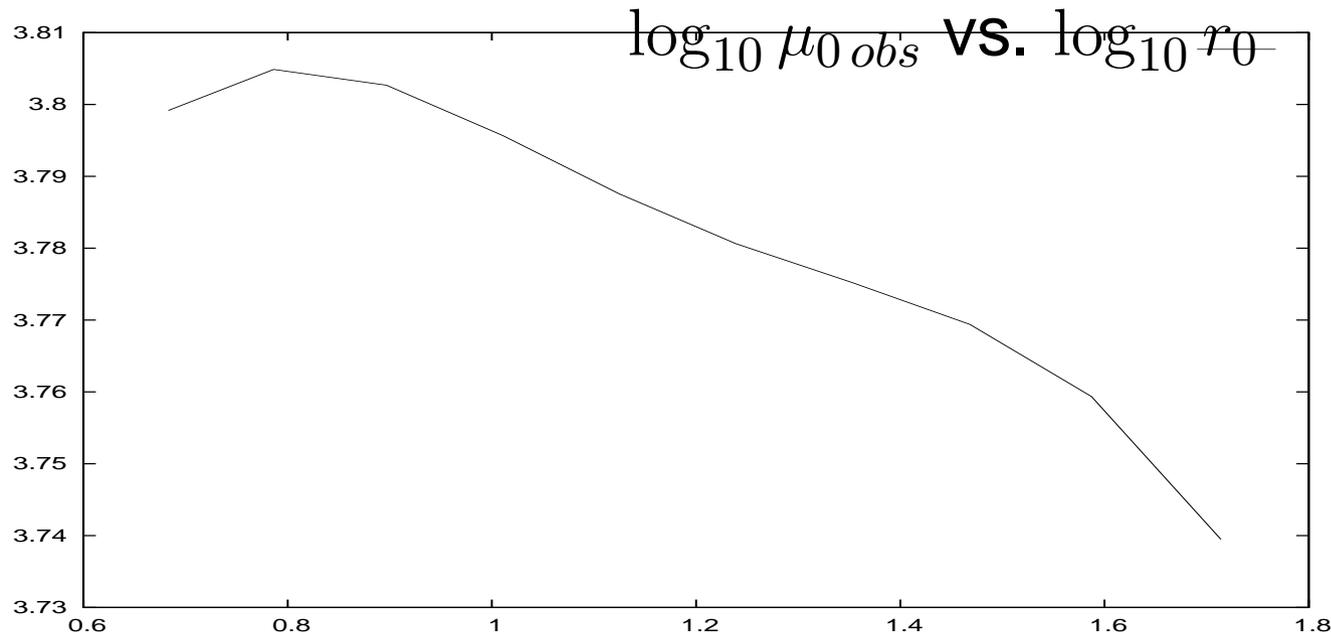# The self-gravity decreasing factor Z for spirals.

$$Q_{today} = \frac{1}{Z}\, Q_{prim} \quad , \quad Q \equiv \frac{\rho}{\sigma^3}$$

$\log_{10} Z$ in solid red line and the common logarithm of the observed phase-space density $\log_{10} Q_{halo}/(keV^4)$ in broken green line vs. $M_{virial}/[10^{11} M_{solar}]$.

The value of Z depends on the type of galaxy.
Z is larger for spirals than for dSphs.

The observed surface density

$$\log_{10} \mu_{0\,obs} \text{ vs. } \log_{10} r_0$$

$\log_{10} \mu_{0\,obs}$ in $(\mathrm{MeV})^3$ vs. the common logarithm of the core radius $\log_{10} r_0$ in kpc from spiral galaxies.

Both r_0 and ρ_0 vary by a factor thousand while μ_0 varies only by about $\pm 10\%$.

Relics decoupling non-relativistic

$$F_d^{NR}(p_c) = \frac{2^{\frac{5}{2}} \pi^{\frac{7}{2}}}{45} \, g_d \, Y_\infty \, \left(\frac{T_d}{m}\right)^{\frac{3}{2}} \, e^{-\frac{p_c^2}{2 \, m \, T_d}} = \frac{2^{\frac{5}{2}} \pi^{\frac{7}{2}}}{45} \, \frac{g_d \, Y_\infty}{x^{\frac{3}{2}}} \, e^{-\frac{y^2}{2 \, x}}$$

$Y(t) = n(t)/s(t)$, $n(t)$ number of DM particles per unit volume, $s(t)$ entropy per unit volume, $x \equiv m/T_d$, $T_d < m$.

$Y_\infty = \frac{1}{\pi} \, \sqrt{\frac{45}{8}} \, \frac{1}{\sqrt{g_d} \, T_d \, \sigma_0 \, M_{Pl}}$ late time limit of Boltzmann.

σ_0: thermally averaged total annihilation cross-section times the velocity.

From our previous general equations for m and g_d:

$$m = \frac{45}{4 \, \pi^2} \, \frac{\Omega_{DM} \, \rho_c}{g \, T_\gamma^3 \, Y_\infty} = \frac{0.748}{g \, Y_\infty} \text{ eV} \quad \text{and} \quad m^{\frac{5}{2}} \, T_d^{\frac{3}{2}} = \frac{45}{2 \, \pi^2} \, \frac{1}{g \, g_d \, Y_\infty} \, Z \, \frac{\rho_s}{\sigma_s^3}$$

Finally: $\qquad \sqrt{m \, T_d} = 1.47 \, \left(\frac{Z}{g_d}\right)^{\frac{1}{3}} \text{ keV}$

We used ρ_{DM} today and the decrease of the phase space density by a factor Z.

Relics decoupling non-relativistic 2

Allowed ranges for m and T_d.

$m > T_d > b$ eV where $b > 1$ or $b \gg 1$ for DM decoupling in the RD era

$$\left(\frac{Z}{g_d}\right)^{\frac{1}{3}} 1.47 \text{ keV} < m < \frac{2.16}{b} \text{ MeV} \left(\frac{Z}{g_d}\right)^{\frac{2}{3}}$$

$g_d \simeq 3$ for $1 \text{ eV} < T_d < 100 \text{ keV}$ and $1 < Z < 10^3$

$1.02 \text{ keV} < m < \frac{104}{b} \text{ MeV}$, $T_d < 10.2$ keV.

Only using ρ_{DM} today (ignoring the phase space density information) gives one equation with three unknowns: m, T_d and σ_0,

$$\sigma_0 = 0.16 \text{ pbarn} \frac{g}{\sqrt{g_d}} \frac{m}{T_d} \qquad \text{http://pdg.lbl.gov}$$

WIMPS with $m = 100$ GeV and $T_d = 5$ GeV require $Z \sim 10^{23}$.

Quantum Fluctuations During Inflation and after

The Universe is homogeneous and isotropic after inflation thanks to the fast and gigantic expansion stretching lenghts by a factor $e^{62} \simeq 10^{27}$. By the end of inflation: $T \sim 10^{14}$ GeV.

Quantum fluctuations around the classical inflaton and FRW geometry were of course present.

These inflationary quantum fluctuations are the seeds of the structure formation and of the CMB anisotropies today: galaxies, clusters, stars, planets, ...

That is, our present universe was built out of inflationary quantum fluctuations. CMB anisotropies spectrum:

3×10^{-32}cm $< \lambda_{begin\ inflation} < 3 \times 10^{-28}$cm

$M_{Planck} \gtrsim 10^{18}$ GeV $> \lambda^{-1}_{begin\ inflation} > 10^{14}$ GeV.

total redshift since inflation begins till today $= 10^{56}$:

0.1 Mpc $< \lambda_{today} <$ 1 Gpc ,   1 pc $= 3 \times 10^{18}$ cm $= 200000$ AU
Universe expansion classicalizes the physics: decoherence

Universe Inventory

The universe is spatially flat: $ds^2 = dt^2 - a^2(t) \, d\vec{x}^2$ plus small primordial fluctuations.

Dark Energy (Λ): 74 % , Dark Matter: 21 %

Baryons + electrons: 4.4 % , Radiation ($\gamma + \nu$): 0.0085%

83 % of the matter in the Universe is DARK.

$$\rho(\text{today}) = 0.974 \; 10^{-29} \; \tfrac{\text{g}}{\text{cm}^3} = 5.46 \; \tfrac{\text{GeV}}{\text{m}^3} = (2.36 \; 10^{-3} \; \text{eV})^4$$

DM dominates in the halos of galaxies (external part).

Baryons dominate around the center of galaxies.

Galaxies form out of matter collapse. Since angular momentum is conserved, when matter collapses its velocity increases. If matter can loose energy radiating, it can fall deeper than if it cannot radiate.

Kinetic Theory in Cosmology

Distribution function in phase-space: $f(t, p_i, x^i)$, $i = 1, 2, 3$

Boltzmann-Vlasov equation:

$$\frac{df}{dt} = \frac{\partial f}{\partial t} + \frac{p^i}{p^0} \frac{\partial f}{\partial x^i} + \frac{dp_i}{dt} \frac{\partial f}{\partial p_i} = \text{Collision terms}$$

Geodesic equations:

$$\frac{dx^\alpha}{dt} = \frac{p^\alpha}{p^0} \quad , \quad \frac{dp_\alpha}{dt} = -\frac{1}{2 \, p^0} \, p_\beta \, p_\gamma \, \frac{\partial g^{\beta \, \gamma}}{\partial x^\alpha} \quad , \quad 0 \le \alpha, \beta, \gamma \le 3$$

The Einstein equations determine the metric $g_{\alpha \, \beta}(t, x^i)$ in terms of the matter+radiation distribution function given by $f(t, p_i, x^i) \Rightarrow$ the Boltzmann-Vlasov equation becomes non-linear.

Collision terms negligible after particle decoupling.

The Boltzmann-Vlasov equation can be linearized around the FRW cosmological geometry before structure formation.